FREQUENCY AND ELECTRIC FIELD DEPENDENT TRANSPORT DUE TO CHARGE DENSITY WAVE CONDENSATES

G. Grüner
Department of Physics
University of California, Los Angeles, CA 90024, U.S.A.

Abstract

Frequency and field dependent transport phenomena associated with charge density wave (CDW) condensates are summarized. Both the ω and E dependent response point to weakly pinned condensates where the characteristic pinning energies are orders of magnitude smaller than the single particle energies. Both classical and quantum description of the CDW dynamics reproduce the main qualitative features of the field and frequency dependent conductivity and dielectric constant, the relation between the parameters which characterize the frequency and field dependent response, and also describe a broad range of experiments which are performed in the presence of joint ac and dc driving fields. Early (unsuccessful) attempts to obtain phonon assisted tunneling and related quantum phenomena are also summarized, together with possible reasons for the failure of such experiments.

CONTENTS

1. INTRODUCTION

The formation of a collective ground state, called the charge density wave (CDW) is well established by structural studies in a broad range of organic and inorganic, low dimensional solids. The term low dimensional refers to the crystal structure which can be viewed as composed of chains or layers of structural units. The strong structural anisotropy also leads to a highly anisotropic electronic band structure. The various instabilities which occur in highly anisotropic metals are understood in detail, and examples for singlet superconducting, spin density wave, and charge density wave ground states have been found in different materials.[1] The CDW ground state which develops below the so called Peierls transition temperature T_P is represented by a periodic lattice distortion and a periodic modulation of the charge density, the latter given by

$$\Delta\rho(x) = \rho_1 \cos(2k_F x+\phi) + \rho_o \qquad (1)$$

where ρ_o is the unperturbed electron density, ρ_1 the amplitude, and ϕ the phase of the condensate. The wavelength λ is related to k_F by $\lambda = \pi/k_F$. The periodic lattice distortion appears in x-ray diffraction patterns; both commensurate ($\lambda = na_o$ with a_o the lattice constant and n integer) and incommensurate ($\lambda \neq na_o$) CDW ground states have been found in various organic and inorganic linear chain compounds.

The establishment of the collective ground state raises the interesting possibility of a new type of collective transport phenomenon, where the response to external dc and ac driving fields is fundamentally different from that of single particle transport. This mechanism was originally suggested by Fröhlich. Early observation of field and frequency dependent conductivity in $NbSe_3$ was followed by a broad range of experiments which demonstrated the highly unusual features of the electrical transport. Similar observations in a rapidly growing number of inorganic chain compounds by now firmly establishes the existence of the new collective transport phenomenon which is largely independent from the details of the underlying single particle effects (such as anisotropy, density of uncondensed electrons, etc.).[2]

While it was argued by Fröhlich that an incommensurate CDW condensate can move unattenuated in the lattice, thus leading to superconductivity, Lee, Rice, and Anderson[3] suggested that various mechanisms, such as interaction between the condensate and impurities and/or the underlying lattice, lead to the pinning of the CDW to particular position in the lattice. The pinning energy per electron can, however, be extremely small, leading to strongly frequency dependent response due to the collective mode at frequencies below the optical

frequency range. This is thought to be responsible for the large dielectric constants and for the structure in the infrared absorption (at energies well below the single particle gap) in materials like the organic donor-acceptor salt TTF-TCNQ or in the inorganic platinum salt KCP.[1] The nonlinear conductivity, which arises when the applied field exceeds a threshold field in $NbSe_3$, together with the anomalous microwave conductivity are, however, the first clear evidences for a collective transport phenomena, carried by the CDW mode. The conductivity was later found to be strongly frequency dependent in the radiofrequency range, with huge low frequency dielectric constant. There is a strong relation between the field and frequency dependent response. This behavior is reproduced by theories which consider classical or quantum processes of the CDW dynamics. With a response which is both nonlinear and frequency dependent, a broad variety of experiments involving both dc and ac driving fields can be performed to test the validity of the various models of CDW transport phenomena. Some of the experimental observations are the straightforward consequence of nonlinear circuit theory. The effect of intrinsic disorder, associated with the randomly positioned impurities, may be responsible for the detailed behavior of $\sigma(\omega)$ and, in particular, to phenomena which occur at low frequencies and long time scales.

In this paper I will discuss the response of the collective mode to external ac and dc driving fields, and survey the main overall featurs of this novel collective transport phenomenon. I will concentrate on the frequency and field dependent response and on the response of the system of joint ac and dc fields. Our observations on the coherent current oscillations and on interference phenomena are discussed elsewhere in this book (see the paper by Professor Zettl). One of the models, the tunneling model, will be reviewed by Professor Bardeen, and therefore in this paper emphasis will be laid on the comparison between the experimental findings and predictions of the so called classical models, where quantum effects associated with the CDW dynamics are neglected.

The phase transitions which led to the development of the CDW ground state together with the evidences for the development of the periodic charge density modulation will not be discussed here. I also refer to recent review papers and other contributions to this book concerning the questions of commensurability, incommensurate-commensurate transitions observed in some materials, etc. Our main concern here is the description of the overall behavior of the collective CDW response observed in a wide range of solids.

The subject has been discussed in several recent reviews,[2] which also cover the various aspects of CDW transport not discussed here.

2. FREQUENCY DEPENDENT CONDUCTIVITY

The frequency dependent response of the coupled electron-phonon system is partially due to excitations across the single particle gap Δ (single particle response), and partially due to the response of the collective mode. The single particle response is that of a semiconductor, where ω dependent conductivity sets in at frequencies $\hbar\omega > \Delta$ with corresponding (small) zero frequency dielectric constant. In the absence of pinning forces the collective mode leads to a strongly peaked response function centered around zero frequency, with a width of the collective mode determined by the damping constant Γ. There is a slight modification of the single-particle response due to a shift of the oscillator strength to zero frequency.

Various pinning effects shift the frequency of the collective mode to finite frequencies. For small pinning forces the oscillator strength associated with the collective mode appears at frequencies $\omega \ll \Delta$, and the response of the collective mode and of single particle effects is well separated. The overall behavior of the ω dependent response expected for an unpinned and pinned CDW system[3] is shown in Fig. 1.

The contribution of the pinned mode to the low frequency dielectric constant was first calculated by Lee, Rice, and Anderson[3] (starting from the Fröhlich Hamiltonian), who find that

$$\varepsilon(\omega) = 1 + \frac{2}{3}\frac{(\hbar\omega_p)^2}{\Delta^2} + \frac{\Omega_p^2}{\omega_o^2 - \omega^2} \tag{2}$$

where the second term is the contribution due to the single particle excitations with $\omega_p^2 = 4\pi ne^2/m$ the plasma frequency, with m the band mass and n the number of electrons, while the third term is the contribution of the collective mode. The effective plasma frequency is

$$\Omega_p^2 = \frac{4\pi\, n_{CDW} e^2}{M^*} \tag{3}$$

with n_{CDW} the number of electrons condensed in the CDW mode, and M* the effective mass of the condensate given by

$$\frac{M^*}{m} = 1 + \frac{1}{g}\frac{\Delta^2}{\hbar^2\,\omega_{ph}^2} \tag{4}$$

where g is the dimensionless electron-phonon coupling constant and ω_{ph} the unrenormalized phonon frequency at $q = 2k_F$. ω_o is a characteristic frequency which represents the strength of the pinning of the collective mode. Damping effects are neglected in the formalism. With damping included in the usual, phenomenological way by introducing a damping constant Γ, the contribution of

the collective mode is given by

$$\varepsilon(\omega) = \frac{\Omega_p^2}{\omega_o^2 - \omega^2 - i\Gamma} \quad .$$

For conventional single particle gaps of the order of 10^{-1} eV the single particles contribution to the dielectric constant is small, and for small pinning forces ε is cominated by the contribution of the collective mode. It is also expected that with $\hbar\omega_o << \Delta$ frequency dependent response occurs at frequencies well below the optical region.

A phenomenological equation of motion which leads to Eq. (2) treats the CDW condensate as an optical mode,[4] and the ω dependent response is that of a harmonic oscillator

$$\ddot{x} + \Gamma\dot{x} + \omega_o^2 x = \frac{e'E}{m'} e^{i\omega t} \tag{5}$$

where e' and m' are the effective charge and effective mass (both included phenomenologically) associated with the response of the condensate, $\omega_o^2 = k/m'$ with k the restoring force. Equation (5) leads to the real and imaginary part of the conductivity

$$\text{Re } \sigma(\omega) = \frac{nee'^2\tau}{m'} \frac{1}{1 + (\omega_{c.o.}/\omega)^2} \tag{6}$$

$$\text{Im } \sigma(\omega) = \frac{nee'^2\tau}{m'} \frac{\omega_{c.o.}}{\omega} \frac{1}{1 + (\omega_{c.o.}/\omega)^2} \tag{7}$$

with the so called crossover frequency $\omega_{c.o.} = \omega_o^2\tau$, and $\tau = \Gamma^{-1}$. The dielectric constant $\varepsilon(\omega)$ is defined as

$$\varepsilon(\omega) = \frac{4\pi \text{ Im } \sigma(\omega)}{\omega} \quad . \tag{8}$$

Figure 2 shows Re $\sigma(\omega)$ and Im $\sigma(\omega)$ for an underdamped ($\omega_o^2\tau << 1$) and for an overdamped ($\omega_o^2\tau >> 1$) response. For an overdamped response Re $\sigma(\omega)$ smoothly increases from zero and at frequences $\omega >> \omega_{c.o.}$ saturates at the value

$$\sigma(\omega >> \omega_o^2\tau) = \frac{nee'\tau}{m'} \quad . \tag{9}$$

The out of phase component has a maximum at $\omega_{c.o.}$ but remains positive in the whole frequency range. In the low frequency, $\omega \to 0$ limit Re $\sigma(\omega) \sim \omega^2$ and Im $\sigma(\omega) \sim \omega$. In case of an underdamped response Re $\sigma(\omega)$ has a maximum and Im $\sigma(\omega)$ a zero crossing at $\omega_{c.o.}$.

Early experiments on the linear chain compound $NbSe_3$ indicated a strongly frequency dependent response[5]: the resistivity anomalies associated with the development of CDW's at 149 K and 59 K are completely removed at microwave (10

GHz) frequencies, as shown in Fig. 3. In orthorhombic TaS_3, where the Fermi surface is completely removed by the Peierls transition and the low field dc conductivity shows a semiconducting behavior below T_p, the microwave conductivity remains high and is orders of magnitude larger tahn the dc conductivity at low temperatures. The dc and high frequency conductivities[6] are displayed in Fig. 4. Strongly frequency dependent response has also been found in other systems which show CDW transport phenomena; in both $(TaSe_4)_2I$[7] and $K_{0.03}MoO_3$[8] the microwave conductivity is much higher than the dc conductivity below the Peierls transition, and is close to the conductivity which would be obtained in the absence of a transition.

Subsequent experiments[9,10] performed in the radiofrequency range show a smooth crossover between the dc and microwave conductivity, with a maximum in the out of phase component around 10^8 Hz. While in the early experiments the conductivity was measured only at a few frequencies, Fig. 5 shows Re $\sigma(\omega)$ and Im $\sigma(\omega)$ in detail. The overall behavior is reminiscent of the overdamped harmonic oscillator response shown in Fig. 2. In fact, a fit to Eqs. (6) and (7) works remarkably well; Fig. 6 shows such a fit[12] for orthorhombic TaS_3 with parameters $\omega_{c.o.} = 160$ MHz and $nee'\tau/m' = 1.1\ \sigma_{dc}$. Using Eqs. (6) and (7) the real and imaginary parts of the conductivity can be combined to give

$$\omega \frac{\text{Re } \sigma(\omega >> \omega_{c.o.})}{\text{Im } \sigma(\omega \to 0)} = \omega_{c.o.} \qquad (10)$$

and from the measured high frequency conductivity and low frequency out of phase component one obtains $\omega_{c.o.} = 277$ MHz which compares favorably with the crossover frequency obtained from the measured frequency dependence. Similar good qualitative account of the experimental data obtained in $NbSe_3$ in both CDW states.[12]

It should be mentioned that the ω dependent response can be also modeled by using conventional passive electronic circuit elements.[13] The ac response can conveniently be described by an RC circuit which, with proper combination of resistances and capacitances, leads to Re $\sigma(\omega)$ and Im $\sigma(\omega)$ which are identical to those given by Eqs. (6) and (7).

The dielectric constant can be evaluated from the measured out of phase component; Eq. (8) together with the measured Im $\sigma(\omega)$ values leads to low frequency dielectric constants in the 10^7 - 10^8 range, enormous values when compared with those obtained in ordinary small band gap semiconductors where ε is of the order of 10. Figures 7, 8, and 9 display the dielectric constant, measured at low frequencies as function of temperature in $NbSe_3$ in orthorhombic TaS_3[14] and in $(TaSe_4)_2I$[15]; the measured threshold electric fields (measured on the same specimens during the same experimental runs) for the onset of nonlinear

conduction (see below) are also displayed in the Figures. Although the conductivity and dielectric constant were found to be frequency dependent even below 1 MHz, ε measured at this frequency is close to the extrapolated, $\varepsilon_1(\omega\to 0)$ value. Therefore we use ε (1 MHz) for ε_o, the static dielectric constant. The rather complicated temperature dependences are not yet understood but we note that, in general, ε appears to be at least qualitatively inversely proportional to the threshold field; this relation will further be discussed later. The giant dielectric constant is in agreement with a small restoring force or with a small characteristic frequency ω_o. The effective mass can be obtained from Eq. (4) with $g \sim 0.25$ (obtained from the mean field expression of the transition temperature), $\Delta \sim 200$ K (appropriate for the lower CDW transition in $NbSe_3$) and $\omega_{2k_F} \sim 100$ K, $M^*/m \sim 10^2$. Then $\varepsilon(\omega\to 0) \sim 10^8$ and Eq. (2) leads with $n \sim 10^{21}$ to $\omega_o \sim 1\times 10^9$ Hz, comparable to the microwave frequency used in experiments displayed in Figs. 3 and 4. Similar values are obtained in orthorhombic TaS_3 and in $(TaSe_4)_2I$.

While the fit to the single harmonic oscillator response shown in Fig. 6 describes rather well the overall behavior of the frequency dependent response, a close inspection of the experimental results reveals serious deviations between this expression and the experiments. This is perhaps most clearly seen by displaying the dielectric constant as function of frequency. Such a plot[15] is shown in Fig. 10 where $\varepsilon(\omega)$ measured in TaS_3 is compared with the harmonic oscillator response. The deviation is most evident at low frequencies. The behavior, displayed in the figure, can in general be represented by a distribution of parameters which determine the ω-dependent response.[16] Such a distribution is not unexpected due to the inherent randomness associated with the randomly positioned impurities which pin the charge density wave. Detailed studies of the frequency and field dependent response in materials with various impurity concentrations clearly demonstrate that pinning is due to impurities, and pinning by commensurability can be neglected even in cases where the CDW is commensurate with the underlying lattice.

The most popular model which treats the pinning of an incommensurate CDW is that of Fukuyama and Lee[17] and of Brasovski[18] who treat the condensate as an elastic medium. The Hamiltonian in one dimension is

$$H = \frac{K}{2}\int dx\left(\frac{d\phi}{dx}\right)^2 + V_o\,\rho_o\sum_i \cos\left(2k_F x_i + \phi(x_i)\right) \quad . \tag{11}$$

The first term represents the elastic energy associated with the local deformations of the charge density wave with K the elastic constant, the second term accounts for the interaction between the condensate and the impurities. It is assumed that the impurity potential is short ranged $V(x) = V_o\delta(x)$, and the

the summation is over all impurity sites i. The number of impurities per unit length is n_i.

Two limits are important. For strong impurities the phase of the CDW is locally fully adjusted to optimize the potential energy gain. The system in this limit can be represented as independent segments each of length $\langle \ell \rangle = 1/n_i$ determined by the average spacing between the impurities. A characteristic pinning frequency is, in this limit, the standing wave oscillation frequency with wavevector $2\pi n_i$. Such arguments lead to

$$\omega_o = 2\pi \, (m/M^*)^{1/2} \, V_F \, n_i \quad . \tag{12}$$

Frequency dependent conductivity occurs where $\omega > \omega_o$. With a random distribution of impurities the characteristic length ℓ between impurities has a distribution given by

$$p(\ell) \sim n_i \exp(-\ell n_i)$$

and a simple average (assuming independent oscillators) leads to a frequency dependent response, which in the limit $\omega \to 0$ is given by

$$\sigma(\omega) \sim \omega^{-2} \exp(-\pi\omega_o/\omega) \quad . \tag{13}$$

Similar expressions have been obtained by Talapov[19] and by Gorkov.[20] In the so called "weak impurity" limit the phase is not adjusted locally to maximize the potential energy gain, but only over a distance L_o given by (in <u>three</u> dimensions)

$$L_o \sim K^2/V_o^2 \rho_o^2 n_i \quad . \tag{14}$$

Fukuyama and Lee argue that $\sigma(\omega) \sim \omega^2$ in this limit, but recent calculations by Feigelman and Vinokur[21] suggest that at low frequencies $\sigma(\omega)$ has the same form as the famous Mott-Berezhinsky law obtained for disordered 1D materials (with electron-electron and electron-phonon interactions neglected)

$$\sigma(\omega) \sim (\omega\tau_{av})^2 \, \ell n^2 \, (\omega\tau_{av}) \tag{15}$$

where τ_{av} is on average relaxation time. Expression (15) is expected to hold when $\omega < \tau_{av}^{-1}$. At very low frequencies Eq. (15) is not appropriate, and can be replaced by Eq. (13).

All of the above approximations are valid only for a strictly one dimensional model such as given by Eq. (11) and, moreover, are expected to be valid only in a restricted frequency range. Therefore we do not compare the experiments with formulas such as given above. Instead, we note that frequency dependent response phenomena observed in random systems are usually analyzed using empirical formulas which often account surprisingly well for the experimental findings. The harmonic oscillator response can be written in the form

a frequency dependent complex dielectric constant

$$\varepsilon(\omega) = \frac{\varepsilon(0)}{1 + i\omega\,\tau_{eff}} \tag{16}$$

where the τ_{eff} relaxation time corresponds to $\tau_{eff} \sim \omega_o^2\tau$. In random systems a modified expression, called Cole-Cole expression[22]

$$\varepsilon(\omega) \sim \frac{\varepsilon(0)}{1 + (i\omega\,\tau_{eff})^{\alpha}} \tag{16a}$$

with $0 < \alpha < 1$ is often used to analyze the experimental findings. This empirical formula can be viewed as representing a distribution of relaxation times τ_{eff} over a broad interval. Equation (14) gives a frequency dependent dielectric constant

$$\text{Re}\ \varepsilon(\omega) = \varepsilon(0)\left[1 - \frac{1}{1 + 2(\omega\tau_{eff})^{-\alpha}\cos\frac{\alpha\pi}{2} + (\omega\tau_{eff})^{-2\alpha}}\right] . \tag{17}$$

A fit to Eq. (17) also shown in Fig. 10 gives a much improved account of $\varepsilon(\omega)$ in a broad frequency range. Similar good fits are obtained for other compounds, with $\alpha \sim 0.7 - 0.8$. Another representation of the experimental findings is in terms of the so called Cole-Cole plot, where Im $\varepsilon(\omega)$ is plotted versus Re $\varepsilon(\omega)$. If Eq. (16a) is valid, then the experimental points are on a semicircle with α determined by the angle between the abscissa and the line which connects the origin to the center of the circle. Such representation, shown in Fig. 12, leads to $\alpha = 0.63$, in good agreement with $\alpha = 0.7$ obtained analyzing the frequency dependent dielectric constant.

In light of the preceding discussion, Figs. 11 and 12 point in general to the importance of randomness in the dynamics of the pinned CDW mode to the distribution of relaxation times which describe the frequency dependent response of the pinned condensate, in terms of the classical Hamiltonian, Eq. (11).

A different line of arguments advanced by Professor Bardeen[23] is also extensively discussed at this Conference. Pinning of the condensate is represented by a gap Δ_p called the pinning gap, and the frequency dependent response arises as the consequence of excitations across the gap. With a gap in the excitation spectrum the dielectric constant in general may be written as

$$\varepsilon = 1 + \frac{4\pi n e^2 \hbar^2}{m\Delta_p^{\,2}} \tag{18}$$

in analogy to the standard expression for the dielectric constant in band semiconductors. The huge low frequency dielectric constant then suggests extremely

small gaps; $\varepsilon = 10^8$ and $n = 10^{21}$ leads to $\Delta \sim 10^{-5}$ K, orders of magnitude smaller than the single particle gaps observed in these materials. Frequency dependent response is also determined by carrier excitations; in general, it is expected that ε increases strongly at frequencies $\omega \sim \Delta_p/\hbar$ and above as observed. The ω dependent response was calculated using expressions appropriate for SIS tunnel junctions, nonlinear elements which also show both frequency and electric field dependent transport phenomena. In the low ac excitation limit a single relation between the ω and E dependent response is observed:

$$\sigma(\omega/\omega_T) = \sigma(E/E_T) \qquad (19)$$

where $\omega_T = \Delta_p/\hbar$ and E_T is a characteristic field where nonlinear conduction sets in and $\sigma = I/E$ is the nonlinear conductivity (see below). This scaling behavior has been shown to be obeyed well both in $NbSe_3$ and in TaS_3, and will be discussed later when experiments in the presence of joint ac and dc excitations are reviewed.

3. ELECTRIC FIELD DEPENDENT CONDUCTIVITY

The strongly nonlinear dc conductivity observed in various materials with a CDW ground state is extensively discussed at this Conference, and there I only shortly summarize the main features of the electric field dependent response. Figure 13 shows $\sigma(E) = I/E$ in orthorhombic TaS_3 well below the Peierls transition temperature. At low electric fields, $E < E_T \sim 300$ mV/cm, current is carried by carrier excitations across the single particle gap and $\sigma_A = I/E$ is ohmic. There is a sharp threshold for the onset of nonlinear conduction above which σ increases dramatically with increasing electric field. The overall functional form of $\sigma(E)$ can be well represented by[25]

$$\sigma(E) = \sigma_A + \sigma_B \left[1 - \frac{E_T}{E}\right] \exp\left[-\frac{E_o}{E}\right] \quad , \qquad (20)$$

first suggested by Fleming and Grimes on empirical grounds.[25] A fit of the experimental[26] data obtained in TaS_3 at various temperatures is shown in Fig. 14. The experimental results displayed in the figure also indicate that temperature driven excitations do not play an important role in determining $\sigma(E)$ -- these certainly would lead to a strongly temperature dependent response, in contrast to what is observed. Equation (20) is also in a broad agreement with the experimental data[2] obtained in $NbSe_3$, NbS_3, and in $(TaSe_4)_2I$. It should also be pointed out that expression (20) leads to a differential conductivity $\sigma_{diff} = dI/dE$, which increases smoothly with increasing electric field. A differential conductivity measured in $NbSe_3$, orthorhombic TaS_3, and other compounds is in agreement with Eq. (20).

The smooth increase of σ when E exceeds E_T is not always observed; a sharp jump of the differential conductance,[27] and hysteresis effects and overshoot phenomena[28] have been widely detected in the various compounds. These phenomena are most probably associated with metastable states which arise as the consequence of local deformations around impurities.

The giant electric constants observed in the materials suggest that the potential energy associated with the pinning of the CDW condensate is extremely small, or alternatively the pinning gap is orders of magnitude smaller than the usual single particle gaps. Broadly speaking, nonlinear conduction is obtained when the energy provided by the applied dc field eEL with L a characteristic length scale is comparable with the energies which charactize the pinning. The observation of strongly non-ohmic conductivity is therefore (in view of the strongly frequency dependent response) not surprising. The models which attempt to describe the frequency dependent response are, however, widely different.

A phenomenological description of the CDW transport[29] treats the CDW as a classical particle moving in a periodical potential, the period given by the CDW wavelength λ. According to the ω dependent conductivity, the inertia term is neglected, and the equation of motion, for a sinusoidal potential $V(\phi) = \omega_o^2(1 - \cos 2k_F x)$ is given by

$$\frac{1}{\tau}\frac{dx}{dt} + \frac{\omega_o^2}{2k_F}\cos(2k_F x) = \frac{e'E}{m'} \quad . \tag{21}$$

Equation (21) leads to a threshold electric field for the onset of nonlinear conduction, and

$$E_T = \frac{m'\omega_o^2\lambda}{2\pi e'} \quad . \tag{22}$$

Above E_T, σ is strongly nonlinear, and the solution for the average velocity $\langle dx/dt \rangle$ in the presence of a constant applied field gives

$$\sigma(E) = \frac{nee'\tau}{m'}\left[1 - (E_T/E)^2\right] , \qquad E > E_T \quad . \tag{23}$$

While the above equation leads to a sharp threshold field and a conductivity which saturates at the high electric field limit, the functional form is in clear disagreement with the experiments. In particular, Eq. (23) leads to a divergent differential conductivity as $E \to E_T$ from above, in clear disagreement with the experiments. The functional form, together with early experimental results, is shown in Fig. 15. The dotted line is expression (23), the full and dashed lines are expresion (20) with different ratios between E_o and E_T.

As mentioned before, a combination of electronic circuit elements are also appropriate for describing the dependent response. This line of approach can be extended to account for nonlinear phenomena. A relaxation oscillator,[13]

based on R and C elements and on a discharge tube or rectifier which breaks down when the applied voltage exceeds a breakdown voltage V_B, also leads to $\sigma(\omega)$ and $\sigma(E)$ which is closely similar to that obtained from Eq. (21), with similar limitations as far as comparison with experiments is concerned.

As discussed earlier, the ω dependent response suggests that disorder associated with the randomly positioned impurities is important, and local deformations of the CDW around the impurities play an important role in the pinning of the charge density wave.

The Hamiltonian given by (11) leads, in the so called weak pinning regime, to an energy gain, due to local adjustment of the phase of the condensate:

$$\Delta E = \frac{V_o^2 \rho_o^2 n_i^2}{K^2} \quad , \tag{24}$$

where n_i is the number of impurities. The energy provided by the dc field applied along the direction of the CDW is described by

$$H_E = \int \frac{e' E_x \phi}{2k_F} dx$$

has to be larger than the pinning energy for sliding CDW to occur. This argument due to Lee and Rice[30] leads to a threshold field for the onset of nonlinear conditions

$$E_T = \frac{\hbar V_F}{8\pi\alpha\, e\, \rho_{eff}\, L_o^2} \quad , \tag{25}$$

Here the change of the internal structure of the CDW by the application of electric field (i.e., dynamics of the internal deformations) is neglected, as in the single classical particle model.

The electric field dependence of the conductivity has been considered by many authors, and the Hamiltonian, given by Eq. (11) supplemented by the term which describes the coupling to the external electric field, Eq. (22) has been solved under various approximations.[31-35] They all remove the divergence in the differential conductivity near threshold and lead to a much improved fit to the experimental data. These approaches are summarized by Dr. Fisher in this Conference.

When tunneling across the pinning gap is considered,[23] a finite threshold field follows from the assumption that the effective field has to be applied across a finite correlation length L to obtain nonlinear conduction. This argument leads to Eq. (20) with

$$E_T = \Delta_p / e^* L \tag{26}$$

and

$$E_o = \Delta_p^2 \pi / 4\hbar V_F e^* \, . \tag{27}$$

Here e* is an effective charge, given by e*/e = m/M (see Bardeen, this Conference). As discussed before, Eq. (20) leads to an excellent account for the observed nonlinear conductivity in $NbSe_3$, TaS_3, and other compounds.

It should be mentioned that none of the above descriptions of the CDW dynamics (except extensions of the Lee-Rice model) can describe a broad variety of phenomena such as switching, hysteresis, and memory effects. These latter are reminiscent of observations made on spin glasses,[36] where local rearrangements of large regions under the influence of magnetic field are responsible for the effects observed. It is expected, therefore, that inclusion of the possibility of local CDW deformations will account for these experimental findings.

4. RELATION BETWEEN THE FREQUENCY AND FIELD DEPENDENT RESPONSE

It is expected that, for a pinned condensate, a strong relation exists between the field and frequency dependent response. In terms of a classical description, both the dielectric constant and the threshold field are related to the restoring force. Alternatively, both $\sigma(\omega)$ and $\sigma(E)$ are related to the pinning gap Δ_p. The strong relation between parameters which characterize the ω and E dependent conductivity has early been recognized, both when different materials and when the same compound with various impurity concentrations are examined. While various parameters, which enter into the expressions on the E dependent response, can be examined, here we compare the low frequency dielectric constant and the threshold field.

In terms of the classical model,[29] Eqs. (8) and (22) lead to

$$\varepsilon_o E_T = 2ne\lambda \quad . \tag{28}$$

The total number of electrons $n = n_\parallel n_\perp$ where $n_\parallel = 2k_F/\pi$ is the number of electrons per unit length and $n_\perp$ is the number of chains per unit cross section. With $\lambda = \pi/k_F$, $n_\parallel e\lambda = 2e$, and

$$\varepsilon_o E_T/n_\perp = 4e \quad . \tag{29}$$

The Fukuyama-Lee-Rice[30] model leads to a static dielectric constant

$$\varepsilon_o = \frac{4\pi ne^2}{m} \frac{\alpha^{4/3}\, c\, L_o^2}{v_F^2} \quad , \tag{30}$$

where c and α are numerical factors of the order of unity,[30] v_F is the Fermi velocity, and L_o is the characteristic length which determines the range of phase coherence [see Eq. (14)]. A coherent region, determined by L_o, is called the Lee-Rice domain. L_o can be estimated using typical values for the Fermi

velocity, for the electrostatic potential V_o and other parameters involved. Such estimations lead to $L_o \sim 10^{-2}$ cm for typical residual impurity concentrations of the order of 100 ppm. Comparing Eqs. (25) and (30)

$$\varepsilon_o E_T / n_\perp = 0.48\ e \quad , \tag{31}$$

while in terms of the semiconductor model [see Eqs. (17) and (27)]

$$\varepsilon_o E_o / n_\perp = 2\pi e \quad . \tag{32}$$

The threshold electric field E_T is of the same order of magnitude, but smaller than E_o, and available experiments are in agreement with $E_o/E_T \sim 5$ for orthorhombic TaS_3 and ~ 2 for $NbSe_3$.[2] With the value appropriate for TaS_3

$$\varepsilon_o E_T / n_\perp = 1.2\ e \quad . \tag{33}$$

All of the above arguments are appropriate in the low temperature $T \to 0$ limit. Temperature dependent effects are expected to enter through the temperature dependent effective charge, associated with the temperature dependence of the condensed electrons. Available experiments, shown in Figs. 7 to 9, do not give a clear indication of the importance of temperature dependent effects. In TaS_3, while both E_T and ε have a well defined temperature dependence, the product $\varepsilon_o E_T$ is independent of T. In $(TaSe_4)_2I$, $\varepsilon_o E_T$ decreases with increasing temperature, and resembles temperature dependent order parameter. More complicated behavior is found in $NbSe_3$ below $T_2 = 59$ K where $\varepsilon_o E_T$ has a maximum close to the maximum of the resistivity (see Fig. 7).

In Fig. 16, ε_o^{-1} is plotted[37] versus $E_T/n_\perp$, with $n_\perp$ obtained from the known crystal structures. The various data for TaS_3 correspond to materials of different purity. In all cases ε_o and E_T values measured well below the transition temperatures were used where $\varepsilon_o E_T$ is approximately independent of temperature. For $NbSe_3$ below T_2, values obtained at T = 42 K were used. It is evident from the figure that $\varepsilon_o E_T / n_\perp$ is approximately constant for all materials investigated thus far. The full line corresponds to

$$\varepsilon_o E_T(\mathrm{exp}) / n_\perp = 0.5\ e \quad , \tag{34}$$

in good agreement with values obtained from the various models. While no distinction between the various models can be made on the basis of the experimentally determined products of $\varepsilon_o E_T$, the overall agreement strongly argues for the close relation between the CDW response to small and large amplitude excitations.

5. EXPERIMENTS IN THE PRESENCE OF JOINT AC AND DC EXCITATIONS

The field and frequency dependent conductivities discussed before represent the behavior of the nonlinear system in two limits. The dc conductivity is regarded as the $\omega \to 0$ limit, while the ac response samples the system in the $E \to 0$ limit. A broad variety of complicated phenomena are expected to occur for finite electric fields applied at finite frequencies which can be perhaps most conveniently analyzed using phase-space plots, as done by Ong and co-workers. Also, dc and ac fields of various magnitudes can be applied to the specimen with the applied voltage

$$V = V_{dc} + V_{ac} \cos \omega t \quad , \tag{35}$$

and the dc and/or ac response can be detected under various circumstances. One class of experiments examines the overall behavior of the nonlinear system in a broad ω, V_{dc}, and V_{ac} parameter space. In a second group belong experiments which search for genuine quantum phenomena such as photon assisted tunneling, while experiments on interference effects[38] between the applied radiation and the intrinsic oscillation belong to the third group. The latter are summarized by Professor Zettl in this Conference.

5.1 Effects associated with the nonlinear response

Two experiments which study the nonlinear response of the system and can be analyzed in terms of various models will be discussed. The first is the effect of ac radiation on the dc response.[39,40] The second is the effect of dc driving field on the dynamical behavior. In the first experiment V_{dc} is a constant and $V_{ac} << V_T$, the threshold voltage for nonlinear conduction, and V_{ac} and ω are varied. The detected quantity is I_{dc}, the time averaged dc current. The dc conductivity $\sigma_{dc} = I_{dc}/V_{dc}$ detected for various ac amplitudes at various frequencies is shown in Fig. 17. The full lines connect points for the same applied ac frequency. The dc threshold electric voltage, measured in the absence of applied ac field was $V_T = 70$ mV. When $V_{dc} + V_{ac} < V_T$ no excess dc conductivity is observed, but σ_{ac} strongly increases with increasing V_{ac} for $V_{dc} + V_{ac} > V_T$. The increase is smaller for larger frequencies. Similar data have been observed in TaS_3.[40] From Fig. 17 one can evaluate the ac amplitude required to produce 1% or 2% increase in σ_{dc} as the function of frequency. A strong increase in V_{ac} is observed at higher frequencies, as seen in Fig. 18. The frequency where this is important coincides with the crossover frequency $\omega_{c.o.} = \omega_o^2 \tau$ as observed in the ac response.

These results are easily explained in terms of the classical model of CDW transport. For a strongly damped CDW system the displacement cannot follow the

ac field at higher frequencies, and consequently larger and larger ac amplitudes are required to lead to the same critical displacement for which dc conduction occurs. From the overdamped harmonic oscillator equation

$$\frac{1}{\tau}\frac{dx}{dt} + \omega_o^2 x = \frac{e'E}{m'} e^{i\omega t} \quad , \tag{36}$$

it follows that the maximum displacement for the CDW is given by

$$x_o = \frac{(e'E/m)\ \omega_o^{-2}}{\left[1 + (\omega/\omega_o^2\tau)^2\right]^{1/2}} \quad . \tag{37}$$

Setting x_o equal to a critical displacement x_{crit} = const. yields a critical ac field amplitude required to lead to a displacement x_{crit}

$$E_{crit}(\omega) = E_{crit}(\omega=0)\left[1 + (\omega/\omega_o^2\tau)^2\right]^{1/2} \quad . \tag{38}$$

The ac amplitude V_{ac} which leads to an enhanced dc conductivity thus increases with increasing frequency, with a crossover from weakly frequency-dependent $V_{ac\ crit}$ to strongly frequency-dependent $V_{ac\ crit}$ around $\omega = \omega_o^2\tau$, which is equal to the crossover frequency for the pure ac response, as discussed earlier. The full line in Fig. 18 is Eq. (38), with parameters given in the Figure caption. These parameters are consistent with those determined separately from the field dependence of $\sigma_{dc}(E)$ and the frequency dependence of $\sigma_{ac}(\omega)$; the difference is not surprising in the light of the qualitative nature of the arguments advanced. Similar good agreement is obtained for TaS_3 and for other materials.

In the second type of experiment the ac response is measured in the presence of a dc driving field, under conditions $V_{ac} \ll V_T$. Figure 19 shows the low frequency dielectric constant[61] as a function of V_{dc}. $\varepsilon(\omega \ll \omega_o^2\tau)$ is independent of V for $V < V_T$ and decreases beyond threshold and approaches zero for $V \to \infty$. The dielectric response which is independent of the ac driving field for $V < V_T$ is in clear contrast to the single particle description. As V_{dc} increases from zero, the polarizability increases, and at $V = V_T$ the restoring force is zero, suggesting an infinite dielectric constant. The functional dependence of the small amplitude dielectric constant can be calculated for a sinusoidal potential, leading to

$$\varepsilon_o(E_{dc}) = \varepsilon_o(E_{dc}=0)\ \left[1 - (E/E_T)\right]^{-1/2} \tag{39}$$

i.e., ε_o diverges as E approaches E_T from below. ε is, however, independent of the applied dc field in the case of a parabolic potential. The insensitivity

of the ac response to the applied dc field is observed at all frequencies. Figure 20 shows $\varepsilon(\omega)$, measured on another specimen for various applied dc fields.

When V_{dc} exceeds the threshold field, ε smoothly decreases with increasing applied dc field, suggesting the gradual loss of polarization. While the ac response for the current carrying condensate, with equation of motion described by Eq. (21), can most probably be evaluated by numerical calculations, simple qualitative arguments, however, can account well for the observed $\varepsilon_o(E_{dc})$ in the nonlinear conductivity regions.

5.2 Search for quantum phenomena associated with the CDW dynamics.

As discussed before, a small effective pinning gap accounts for the giant dielectric constant and for the large nonlinear dc response for small electric fields, with a relation between the ω and E dependent response similar to that obtained from a classical dynamics. The frequency dependent response calculated using the formalism developed by Tucker[42] for SIS junctions leads to Eq. (19), and the scaling behavior for $NbSe_3$ is shown in Fig. 21. $\sigma(0,E)$ refers to the dc response as the function of applied field, $\sigma(\omega,0)$ is the ac response for small electric fields. The scaling behavior is also observed in $NbSe_3$ below the second CDW transition for ($T < T_p = 59$ K). This is shown in Fig. 22. In contrast to the sharp threshold field E_T there is no sharp threshold frequency, and the ω dependent response starts at $\omega = 0$. This behavior is discussed by Professor Bardeen in this Conference.

The formalism which leads to Eq. (19) can also be used to calculate the dc conductivity in the presence of applied ac field. With $\sigma(E)$ described by Eq. (20) and $\sigma(\omega)$ obtained from the scaling arguments, σ_{dc} curves can be generated by computer. A fit[44] of σ_{dc} conductivity measured in the presence of applied ac fields is shown in Fig. 23. Similarly, the dependence of the dielectric constant or the applied dc field can also be accounted for by the formalism.[45]

According to the tunneling model of CDW transport, the energy provided by the applied ac and dc field can be combined to lead to dc conductivity. With the characteristic length L discussed before, the energy associated with the dc field is eEL, and the conditions for ac induced dc conduction (corresponding to photon assisted tunneling) are

$$eE_{dc}L + \hbar\omega > eE\,L$$

$$E_{dc} + E_{dc} < E_T \qquad (40)$$

Tucker's formalism[42] leads to a dc current

$$\Delta I_{dc}(\omega) = \frac{eV_{ac}}{2\hbar\omega}\left[I_{dc}\left(V_{dc}+(\hbar\omega/e)\right) + I_{dc}\left(V_{dc}-(\hbar\omega/e)\right) - 2I_{dc}(V_{dc})\right] . \qquad (41)$$

All the parameters appearing in the equations can be measured during the experiments. No excess dc current was detected[43] for various combinations of dc and ac driving fields (i.d., for various combinations of $V_{dc} \pm (\hbar\omega/e)$), and we conclude that photon assisted tunneling, *from the pinned to the current carrying state*, does not occur in the materials $NbSe_3$ and TaS_3 investigated so far.

6. THE HIGH FREQUENCY AND HIGH FIELD LIMIT OF THE CDW CONDUCTION

It was noted earlier that the conductivity which occurs at high electric fields and high frequencies in $NbSe_3$ is similar in magnitude to σ which would be obtained in the absence of the transition to the CDW ground state. Arguments why this may occur have been advanced by Bardeen[23] and by Gorkov and Dolgov.[46]

In Fig. 24 we show high frequency and high field conductivity data[47] on TaS_3 and on an alloy $Ta_{1-x}Nb_xS_3$ with $x = 0.1\%$. Similar results have been obtained recently in TaS_3 samples subjected to neutron irradiation. The dotted line is the dc conductivity of $TaSe_3$, a material which does not undergo a Peierls transition and remains metallic down to low temperatures. Experiments performed at 9 and 35 GHz gave similar results, confirming that the microwave conductivity data shown in the figure correspond to the high frequency $\omega >> \omega_o^2\tau$ limit. The high field $E \to \infty$ data were obtained by extending the dc conductivity measurements to very high ($E \sim 100\ E_T$) electric fields. Fits to various expressions of the measured $\sigma(E)$ lead to the same high field conductivity within experimental error. There are several important conclusions which can be drawn from the experimental data presented in Fig. 24. First, the high field and high frequency conductivity is the same. This is expected on the basis of both the tunneling and classical description; in both cases $\sigma(E \to \infty)$ and $\sigma(\omega >> \omega_{c.o.})$ can be written as

$$\sigma(E \to \infty,\ \omega >> \omega_o^2\tau) = \frac{nee^*\tau}{m^*} \tag{42}$$

where e^* and m^* (or alternatively e' and m') are the effective mass and charge of the condensate. The fact that experimentally the two quantities are the same strongly suggests that the relaxation time (or damping constant) is the same for small amplitude oscillations and for sliding motion of the condensate. Second, although the high frequency or high field conductivity is not the same as σ, which would be obtained in the absence of CDW transitions, it is within the same order of magnitude. As the usual conductivity is given by $\sigma = ne^2\tau_n/m$, this implies that

$$\sigma(E \to \infty,\ \omega >> \omega_o{}^2\tau) = \frac{nee^*\tau_{eff}}{m^*} \tag{43}$$

where τ_{eff} is an effective relaxation time which limits the conductivity at high frequencies and at high electric fields. It is also evident from the figure that impurities play an extremely important role in limiting the CDW conduction. 0.1% Nb impurity concentration has certainly a negligible effect on the conductivity due to the normal electrons. In contrast to this the CDW is depressed by more than an order of magnitude by such amount of (weakly scattering) impurities. While similar experiments performed on TaS_3 samples with slightly different residual impurity concentrations (as confirmed by the measurements of the threshold electric field) led to high frequency or high field limits which were the same within experimental error, it is not clear whether τ is determined by impurities or by interactions with phonons or normal electrons for low concentration of impurities. Similar conclusions were obtained from studies of $NbSe_3$ and its alloys.[69] The temperature dependence of the high field or high frequency limit is similar to that obtained in $(TaSe_4)_2I$[50] and in $K_{0.3}MoO_3$,[8] and σ strongly decreases with decreasing temperatures in the low temperature ($T < \frac{1}{2} T_p$) region. This behavior [along with other temperature dependent phenomena such as $E_T(T)$ or $\varepsilon_o(T)$], however, is not understood at present.

7. CONCLUSIONS

Considerable progress has been made towards understanding the unusual transport phenomena associated with the dynamical response of the CDW condensate. The main features of the ω and E dependent response are well documented in a broad range of materials with a CDW ground state, and the observed phenomena are independent of the details of the crystal and electronic structure: a clear signature for a collective transport phenomenon.

In spite of a large body of experimental data concerning the ω dependent response of the pinned mode, there is a clear need for the extension of experiments both to lower and to higher frequencies. Studies of the low frequency response, both in the frequency and in the time domain, will clarify the role of metastable states and the area of CDW dynamics which is related to spin glass type of behavior. The high frequency region, including millimeter wave and optical frequencies, may clarify the importance of inertia effects and finite time scales associated with the CDW dynamics and damping. New experiments which include the joint application of ac and dc driving fields may further test the nonlinear response of the system. A detailed study of such phenomena[51] has recently been interpreted in the framework of the tunneling theory, but these calculations should be complemented with computer simulations based on the

classical models of CDW transport.[52] Such calculations, together with experiments performed at high (possibly microwave) frequencies will hopefully clarify the role of quantum processes in the CDW transport.

Some of the experiments reported here were also analyzed in terms of the dynamics of a soliton lattice, which may develop in materials where the CDW is close to commensurability, as in $NbSe_3$. The (phenomenological) solution of the models[53-55] is in general not very different from that worked out for the classical, rigid CDW model, and consequently does not differ much from the $\sigma(E)$ and $\sigma(\omega)$ behavior obtained on the basis of the latter model. On the experimental side, the observed behaviors are rather similar for a broad range of materials, and therefore descriptions in terms of models which have particular requirements concerning the parameters of the CDW are most probably not relevant.

From the discussion of the relation of the ω and E dependent response it is clear that both the classical and the tunneling model lead to similar relations between the parameters involved. The models, however, lead to rather different length scales associated with the coherent CDW. In the single particle model, the CDW wavelength λ plays a fundamental role, while when local deformations are included, the range of phase correlations is given by the length of the so called Lee-Rice domain. In the tunneling model, the characteristic length is related to the pinning gap Δ_p. Direct measurements of these length scales have not been yet successful, but recent experiments on the length dependent threshold field[48] or volume dependent current oscillations[49] indicate coherent regions with characteristic dimensions of the order of 10^{-4} - 10^{-3} cm. Further experiments could firmly establish the magnitude of the length scales involved and thus point to the validity of the various models.

It is also evident that the experiments which involve the joint application of ac and dc driving fields, and were discussed here, represent a small cross section of a broad class of experiments which can be performed in nonlinear systems. Both experiments focus on the small response of the system, assuming (for example) a sinusoidal response in the nonlinear region. This certainly is not the case, and rectification and harmonic mixing phenomena are expected and readily observed[59] in these materials. Bifurcation and turbulent behavior, however, are not expected to occur, mainly because of the overdamped response observed. A combination of the specimens with passive circuit elements, such as inductance, however, may lead to an "underdamped" response and the possibility of turbulent response in the presence of both dc and ac driving fields.

In spite of rapid progress in this area, many experimental and theoretical questions remain, and important new developments are expected in the near future.

8. ACKNOWLEDGMENTS

I have enjoyed pleasant interactions with many colleagues during the course of experiments which are reported here. The experimental work was conducted in collaboration with W. G. Clark, A. Janossy, G. Mozurkewich, A. Zettl, and Wei-yu Wu. The ideas expressed by John Bardeen, T. Holstein, A. M. Portis, J. R. Schieffer, and A. Zawadowski had a major influence on the experiments which were designed and conducted.

This research was supported by NSF grants DMR 81-03085 and DMR 81-21394.

REFERENCES

1. See, for example, Highly Conducting One Dimension Solids, ed., I. T. Devreese (Plenum, New York & London, 1979); A. J. Berlinsky, Rep. Progr. Phys. 42, 1244 (1979); and articles in Molecular Crystals and Liquid Crystals, Vol. 81 (1982).
2. R. M. Fleming, in Physics in One Dimension, Springer Series in Solid State Sciences 23, eds., J. Bernasconi and T. Schneider (Springer Verlag, Berlin, Heidelberg, New York, 1981); P. Monceau, Physica B + C 109, 1890 (1982); N. P. Ong, Can. J. Phys. 60, 757 (1981); G. Grüner, Comments in Solid State Physics 10, 173 (1983); G. Grüner, Physica D 262 (1983) (to be published).
3. P. A. Lee, T. M. Rice, and P. W. Anderson, Solid State Comm. 14, 703 (1974).
4. M. Rice, in Low Dimensional Cooperative Phenomena, ed., U. J. Keller (Plenum Publishing Co., New York, 1975).
5. N. P. Ong and P. Monceau, Phys. Rev. B 16, 3443 (1977).
6. C. Jackson, A. Zettl, G. Grüner, and A. M. Thompson, Solid State Comm. 39, 532 (1981); similar data have been obtained by N. P. Ong, et al., Mol. Cryst. Liq. Cryst. 81, 41 (1982).
7. M. Maki, M. B. Kaiser, A. Zettl, and G. Grüner, Solid State Comm.
8. D. Reagor, G. Mozurkewich, and L. Schneemeyer (to be published).
9. G. Grüner, L. C. Tippie, J. Sanny, W. G. Clark, and N. P. Ong, Phys. Rev. Lett. 45, 935 (1980).
10. S. W. Longcor and A. M. Portis, Bull. Am. Phys. Soc. 25, 340 (1980); J. C. Gill, Solid State Comm. 37, 459 (1981).
11. A. Zettl, C. M. Jackson, and G. Grüner, Phys. Rev. B 26, 57 (1982).
12. A. Zettl, Thesis, University of California (1983).
13. M. Weger, G. Grüner, and W. G. Clark, Solid State Comm. 49, 1179 (1982).
14. Wei-yu Wu, A. Janossy, and G. Grüner, Solid State Comm. (to be published).
15. Wei-yu Wu (unpublished).
16. A. M. Portis, Molecular Crystals and Liquid Crystals 81, 33 (1982).
17. H. Fukuyama and P. A. Lee, Phys. Rev. B 17, 535 (1978). For a review on

the theory based on the phase Hamilton, Eq. (11), see H. Fukuyama and H. Takayama, to be published in "Electronic Properties of Inorganic Quasi One-Dimensional Compounds," ed., P. Monceau.

18. S. A. Brasovski, Zh. ETF 76, 1000 (1979); see also A. I. Larkin and P. A. Lee, Phys. Rev. B 17, 1596 (1978).
19. A. I. Talapov, Sov. Phys. JETP 54, 1000 (1979).
20. L. P. Gorkov, Pisma Zh. ETF 25, 384 (1977); JETP Lett. 25, 358 (1977).
21. M. V. Feigelman and V. M. Vinokur, Solid State Comm. 45, 599 (1983); M. V. Feigelman, Zh. ETF 79, 1095 (1980); M. V. Feigelman and V. M. Vinokur, Phys. Lett. (1981).
22. For a review of frequency dependent conductivity in random systems, see K. L. Ngai, Comments in Solid State Physics 9, 127 (1979) and references cited therein.
23. John Bardeen, Mol. Cryst. Liq. Cryst. 81, 1 (1982); ibid., Varenne Lecture Notes (1983) and references cited therein.
24. In the model for the CDW pinning, an effective charge $e^*/e = m/M$ is introduced, and this effective charge replaces e in the relevant expressions of the dielectric constant and characteristic field.
25. R. M. Fleming and C. C. Grimes, Phys. Rev. Lett. 42, 1423 (1979); R. M. Fleming, Phys. Rev. B 23, 1567 (1981). The formula suggested on empirical grounds is slightly different from Eq. (17); instead of E_o/E in the exponential, $E_o/(E-E_T)$ appears.
26. A. Zettl, G. Grüner, and A. H. Thompson, Phys. Rev. B 26, 5760 (1982).
27. P. Monceau, J. Richard, and M. Renard, Phys. Rev. B 25, 931 (1982); A. Zettl and G. Grüner, Phys. Rev. B 26, 2298 (1982); G. Hutivay, L. Mihaly, and G. Mihaly, Solid State Comm. (1983).
28. J. C. Gill, Solid State Comm. 39, 1203 (1981); R. M. Fleming, Solid State Comm. 43, 167 (1982).
29. G. Grüner, A. Zawadowski, and P. M. Chaikin, Phys. Rev. Lett. 46, 511 (1981). Some of the details of the model have been worked at by Monceau, et al., Ref. 27, and by E. Ben Jacob, Solid State Comm. (1983) (to be published).
30. P. A. Lee and T. M. Rice, Phys. Rev. B 19, 3970 (1979).
31. L. Sneddon, M. C. Cross, and D. S. Fischer, Phys. Rev. Lett. 49, 292 (1982); L. Sneddon, Phys. Rev. (to be published).
32. D. S. Fischer, Phys. Rev. Lett. 50, 1486 (1983).
33. R. A. Klemm and J. R. Schrieffer, Phys. Rev. Lett.
34. B. Joos and D. Murray (to be published).
35. L. Pietronero and S. Strässler (to be published).
36. This point was stressed recently by R. M. Fleming and L. Schneemeyer on the

basis of observations made on the blue bronze $K_{0.3}MoO_3$.
37. Wei-yu Wu and G. Grüner (to be published).
38. Interference phenomena, first observed by P. Monceau, J. Richard, and M. Renard, Phys. Rev. Lett. 45, 43 (1980), have recently been extensively studied; A. Zettl and G. Grüner, Solid State Comm. (1983); ibid., Phys. Rev. B (1983).
39. G. Grüner, W. G. Clark, and A. M. Portis, Phys. Rev. B 26, 3641 (1981).
40. A. Zettl and G. Grüner, Phys. Rev.
41. G. Grüner, Molecular Crystals and Liquid Crystals 81, 17 (1982).
42. J. R. Tucker, IEEE J. Quant. Electron. 15, 1234 (1979).
43. G. Grüner, A. Zettl, W. G. Clark, and John Bardeen, Phys. Rev. B 24, 7247 (1981).
44. J. R. Tucker, J. M. Miller, K. Seeger, and John Bardeen, Phys. Rev. B 25, 2979 (1982).
45. J. R. Tucker (private communication).
46. L. P. Gorkov and E. N. Dolgov, Zh. Exp. Teor. Fiz. 77, 396 (1979) [Zh. ETP 50, 203 (1979)].
47. A. Janossy, Pei-Ling Hsieh, and G. Grüner (to be published).
48. G. Mihaly (private communication).
49. M. Oda and M. Ido, Solid State Commun. 44, 1535 (1983).
50. D. Reagor (to be published).
51. J. M. Miller, J. Richard, J. R. Tucker, and John Bardeen (to be published).
52. Such type of calculations, performed recently by W. Wonneberger, are also in good qualitative agreement with the experimental data.
53. M. Weger and B. Horowitz, Solid State Commun. 43, 583 (1982).
54. M. Imada, J. Phys. Soc. Japan 50, 401 (1981).
55. B. Horowitz and S. Trullinger, J. de Physique (to be published).

FIGURE CAPTIONS

Fig. 1. Frequency dependent conductivity for an a) unpinned and b) pinned CDW condensate. Δ refers to the single particle gap.

Fig. 2. Real and imaginary parts of the conductivity Re $\sigma(\omega)$ and Im $\sigma(\omega)$ as calculated for an overdamped and underdamped harmonic oscillator.

Fig. 3. Temperature dependence of the dc and microwave conductivity in $NbSe_3$.

Fig. 4. Dc and microwave conductivity in orthorhombic TaS_3. The Peierls transition T_p at 215 K is evidenced by the sharp temperature derivative of σ.

Fig. 5. Re $\sigma(\omega)$ and Im $\sigma(\omega)$ in $NbSe_3$ at T = 42 K.

Fig. 6. Re $\sigma(\omega)$ and Im $\sigma(\omega)$ measured for TaS_3 at T = 210 K. The solid and dotted lines are fits to the classical overdamped oscillator model with parameters given in the text.

Fig. 7. Temperature dependence of the low frequency (f = 20 MHz) dielectric constant and threshold electric field in $NbSe_3$.

Fig. 8. Temperature dependence of the low frequency (f = 1 MHz) dielectric constant and threshold electric field in orthorhombic TaS_3. The temperature dependence of $\varepsilon_o E_T$ is also shown in the Figure.

Fig. 9. Temperature dependence of the low frequency (2 MHz) of the dielectric constant in $(TaSe_4)_2I$. The product $\varepsilon_o E_T$ is also shown in the figure.

Fig. 10. Frequency dependent dielectric constant of orthorhombic TaS_3. The dashed line is the prediction of the harmonic oscillator description and the full line is a fit to Eq. (17) with $\omega_{c.o.}$ = 29 MHz, $\varepsilon(0) = 3.9\times10^7$, and α = 0.7.

Fig. 11. Frequency dependent dielectric constant is $NbSe_3$, TaS_3, and $(TaSe_4)_2I$ at various temperatures.

Fig. 12. Cole-Cole plot for the complex dielectric constant of TaS_3. The

numbers above some data points refer to the frequencies of the measurements.

Fig. 13. Electric field dependence of the dc conductivity $\sigma = I/V$ in orthorhombic TaS_3. σ_{RT} refers to the room temperature conductivity. For $\sigma(E)$ at various temperatures, see Ref. 26.

Fig. 14. Field dependence of the nonlinear conducting $\sigma(V) - \sigma(V \to 0)$ at three different temperatures. The full line is fit to Eq. (20) with parameters given on the figure.

Fig. 15. Nonlinear conductivity in $NbSe_3$ and the functional forms of $\sigma(E)$ obtained from the various models. The dotted line is Eq. (20); the other curves are Eq. (20) with parameters given in the Figure.

Fig. 16. Inverse dielectric constant versus threshold electric field. The full line corresponds to $\varepsilon E_T/n_\perp = 0.5$ e.

Fig. 17. Normalized dc conductivity as a function of applied ac amplitude, for various frequencies.

Fig. 18. Frequency dependence of the ac amplitude which leads to an excess dc conductivity 1% and 2% larger than the $\sigma(V \to 0)$ value. V_T refers to the threshold voltage for dc nonlinearity. The solid curve is Eq. (36) with parameters $V_{ac}(\omega = 0) = 0.14$ V and $\omega_{c.o.}/2\pi = 50$ MHz.

Fig. 19. Low frequency (5 MHz and 20 MHz) dielectric constant as a function of applied dc bias. The dc conductivity, $\sigma(V)$, is also shown in the Figure.

Fig. 20. Frequency dependent dielectric constant measured at various applied dc applied fields below and around E_T.

Fig. 21. Field (upper scale) and frequency (lower scale) dependent conductivity in $NbSe_3$ at T = 130 K. The full and dotted lines are Eq. (20) with parameters given on the Figure. The scale has been adjusted to demonstrate the scaling observed for $V > 2\ V_T$.

Fig. 22. Field (lower scale) and frequency (upper scale) dependent response in $NbSe_3$ at T = 42 K.

Fig. 23. Ac induced dc conductivity calculated on the basis of the tunneling model (full lines). The experimental data are the same as those shown in Fig. 17.

Fig. 24. The high field ($E \to \infty$) and high frequency ($\omega >> \omega_o^2\tau$) limits of the CDW conductivity in TaS_3 and its alloys.

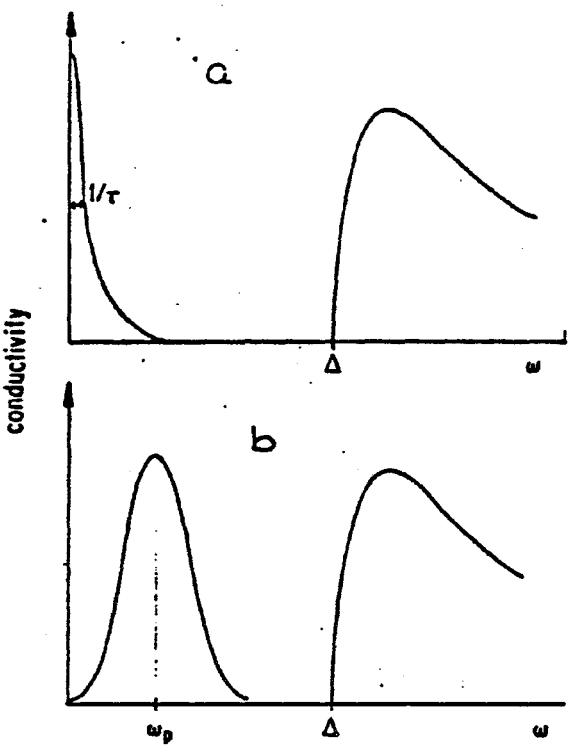

Figure 1

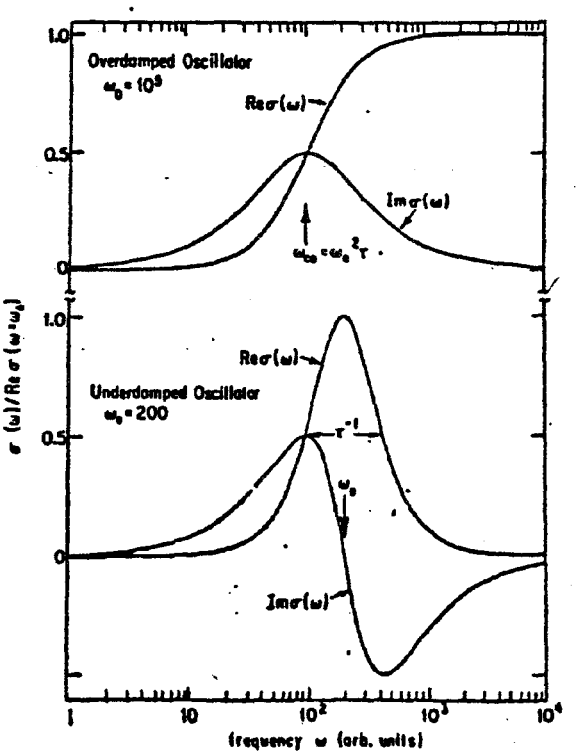

Figure 2

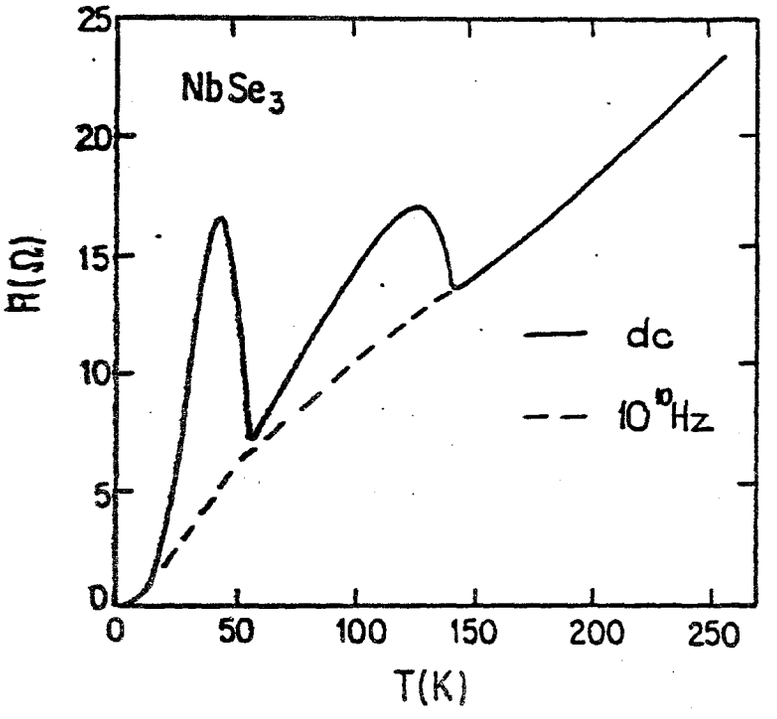
NbSe3
R(Ω)
T(K)
dc
10^n Hz
0
5
10
15
20
25
0
50
100
150
200
250

Fig 3

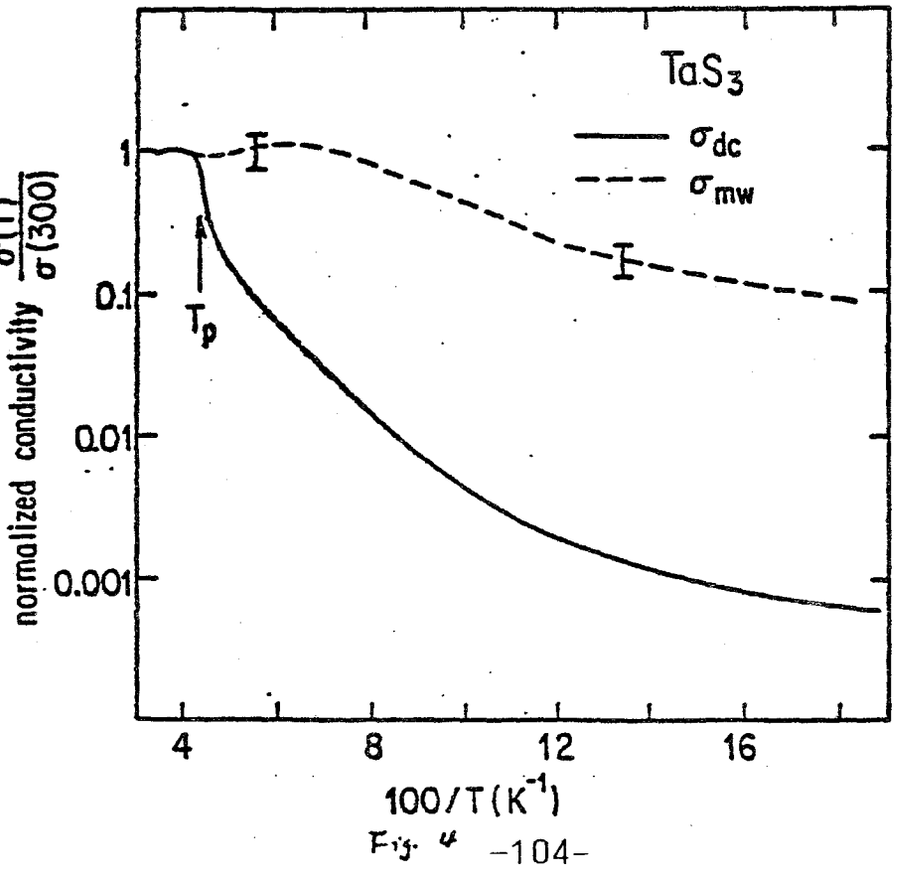
TaS3
σdc
σmw
Tp
normalized conductivity σ(T)/σ(300)
100/T(K^-1)
1
0.1
0.01
0.001
4
8
12
16

Fig. 4

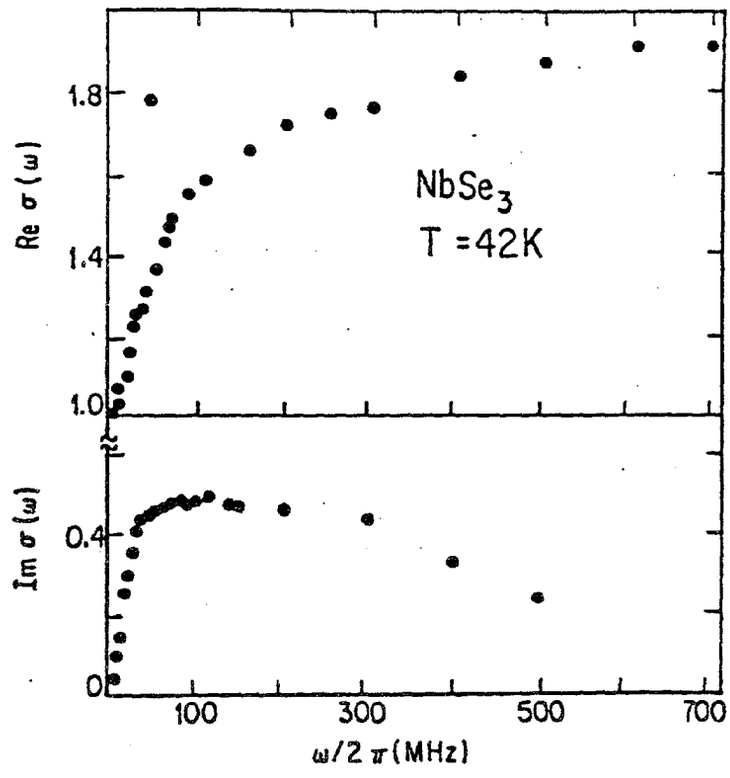

Figure 5

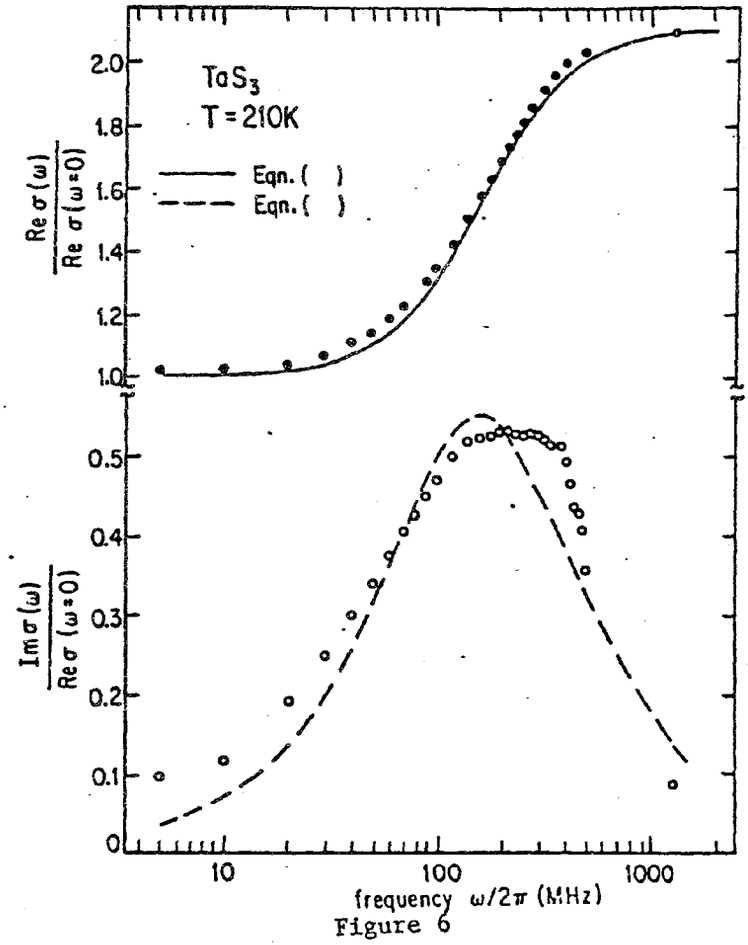

Figure 6

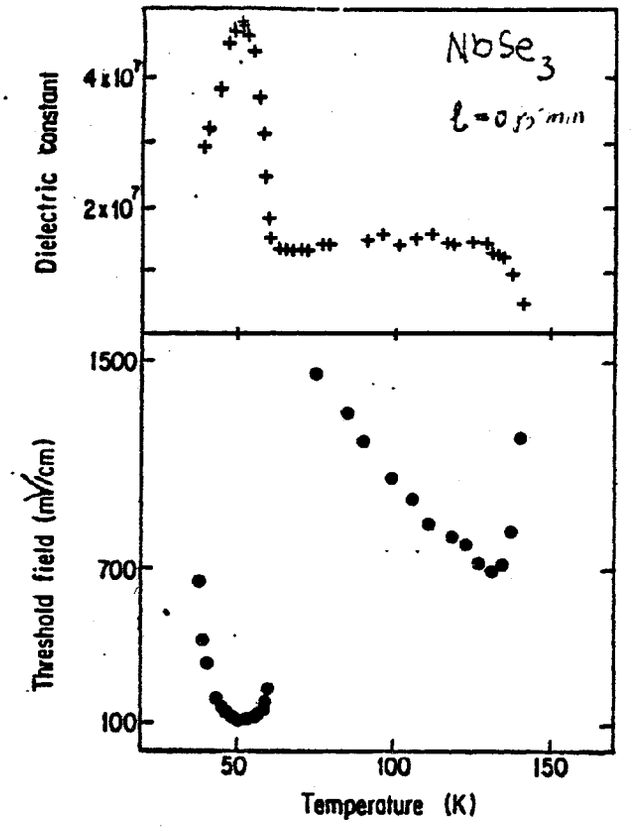

Figure 7

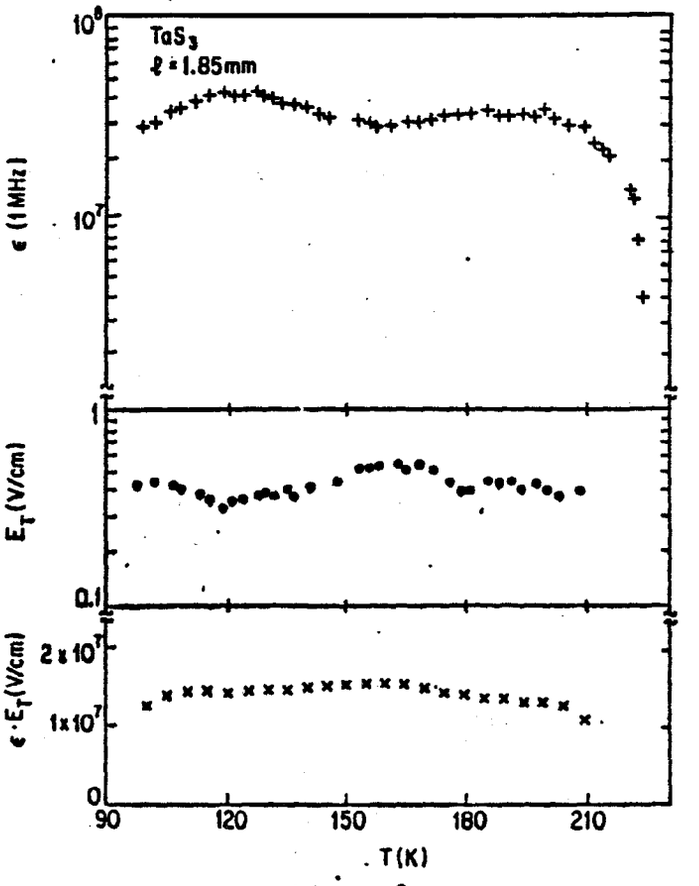

Figure 8

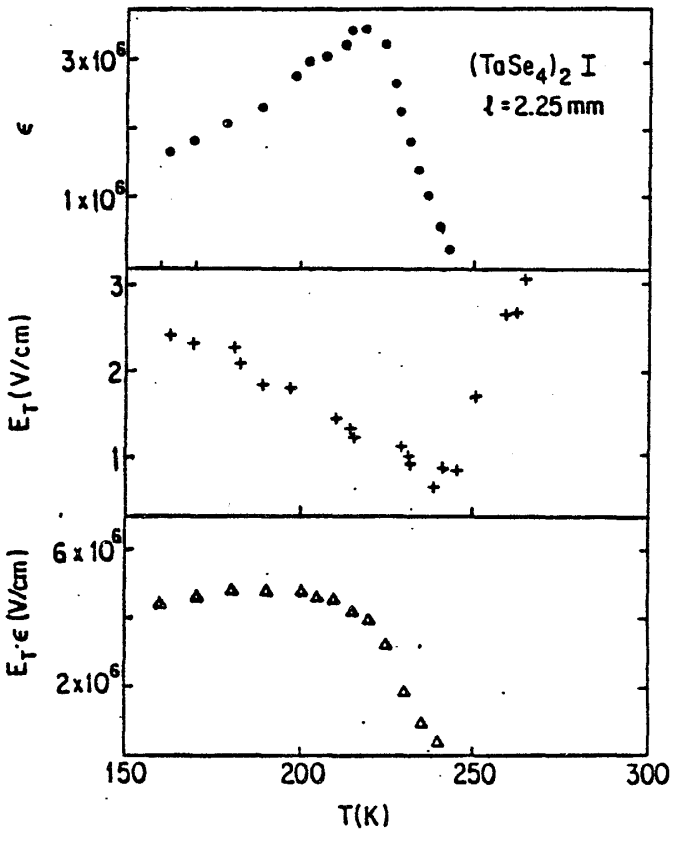

Figure 9

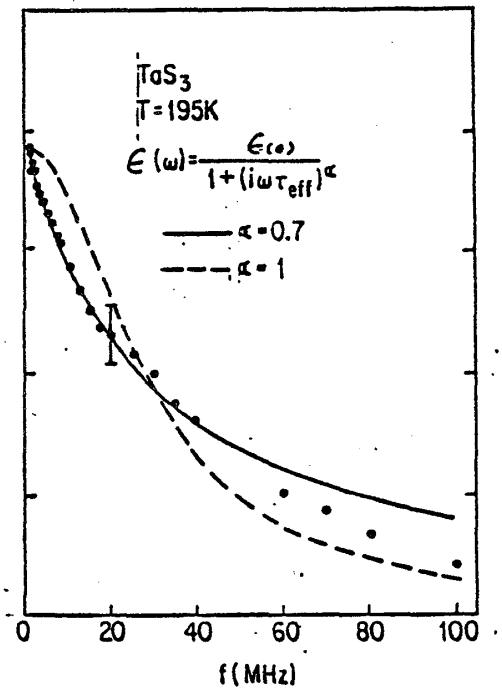

Figure 10

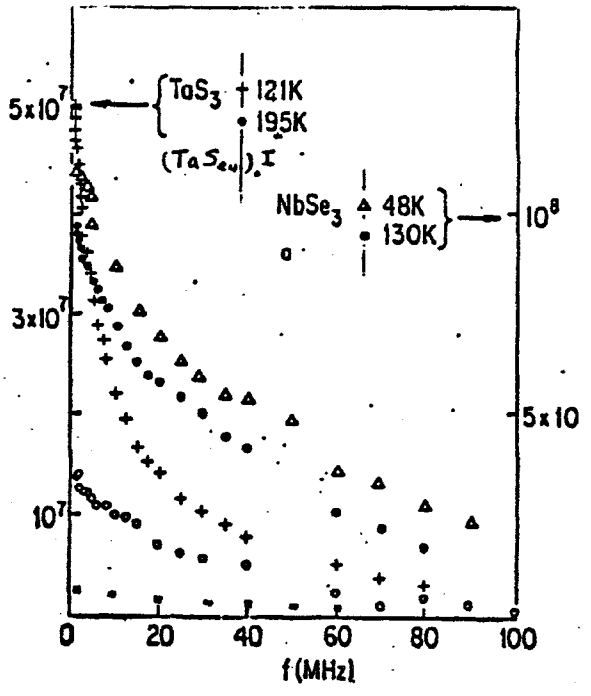

Figure 11

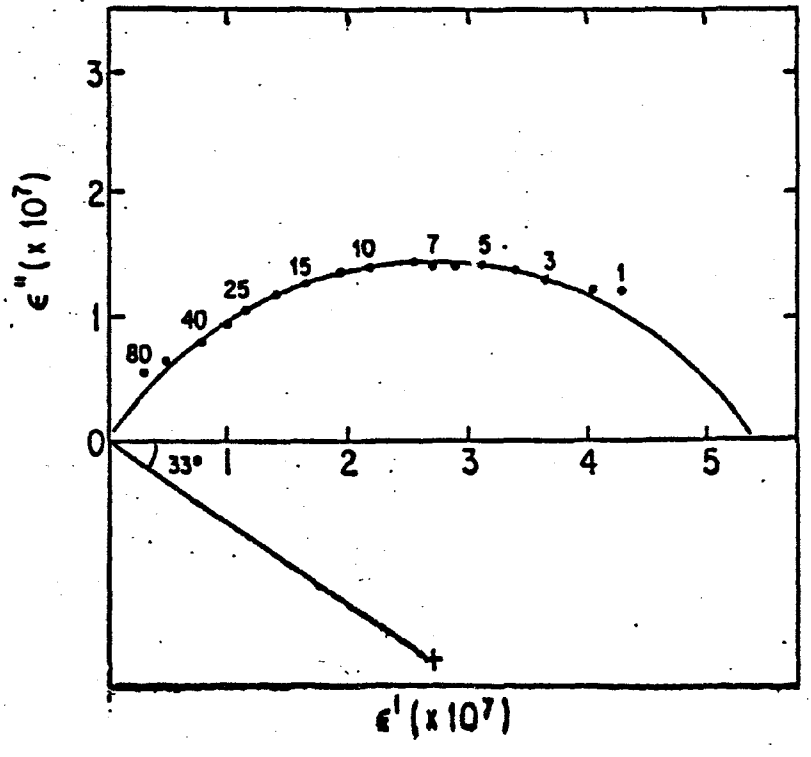

Figure 12

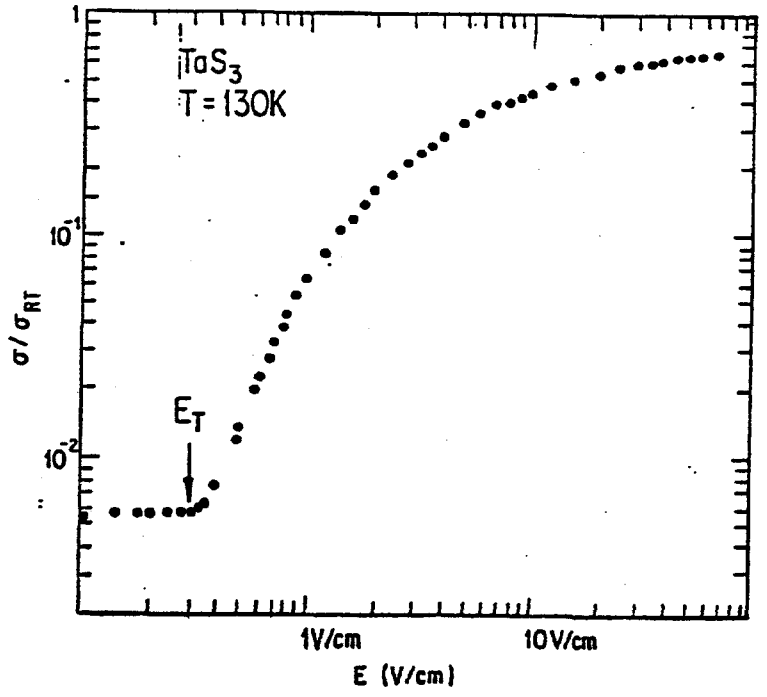

Figure 13

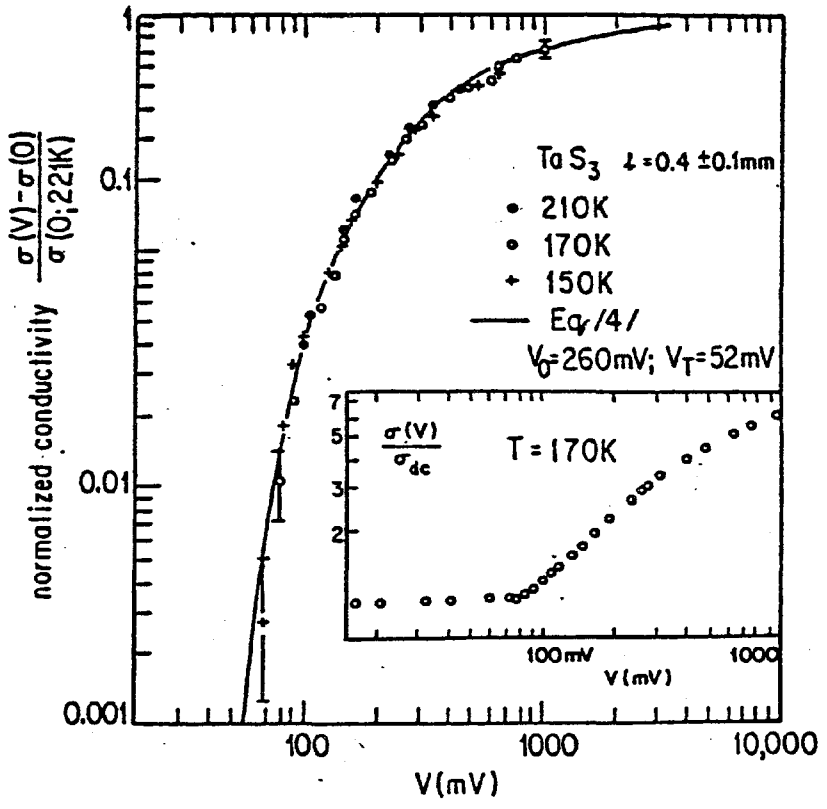

Figure 14

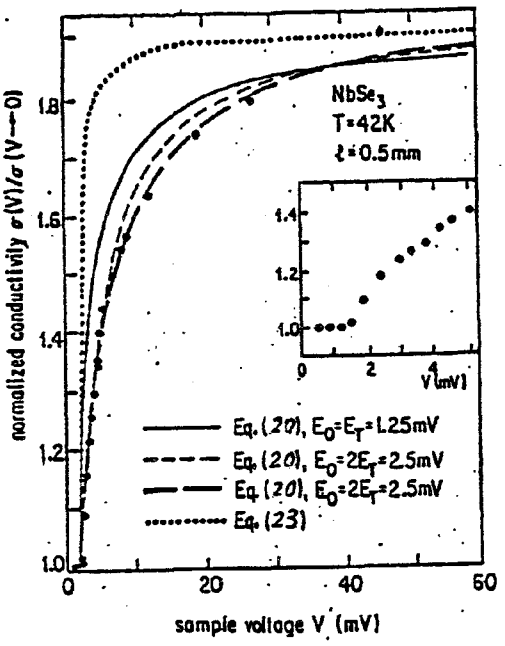

Figure 15

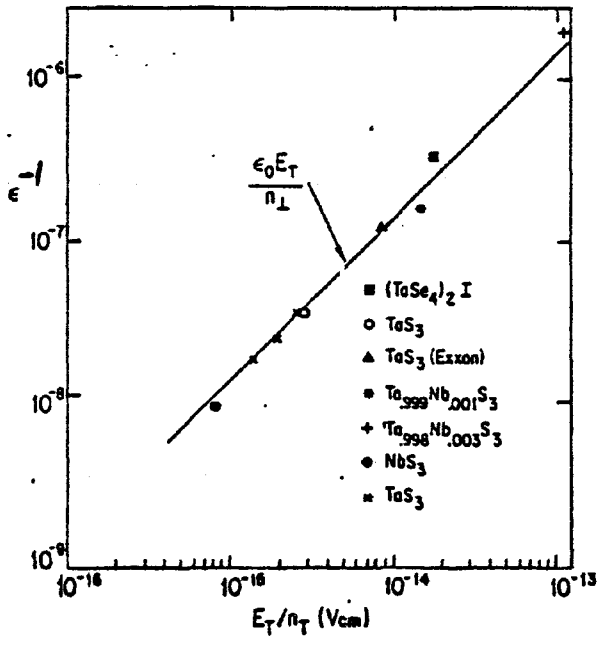

Figure 16

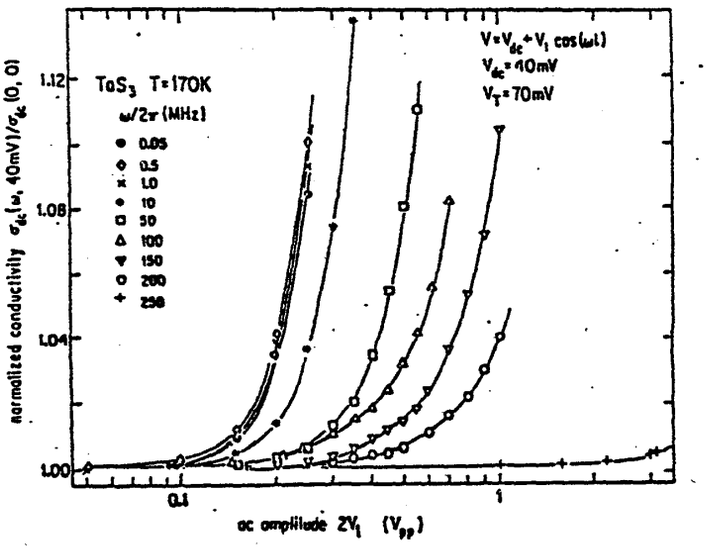

Figure 17

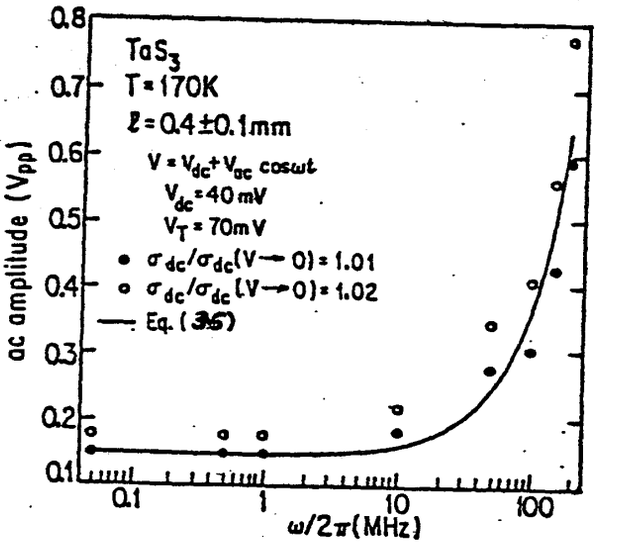

Figure 18

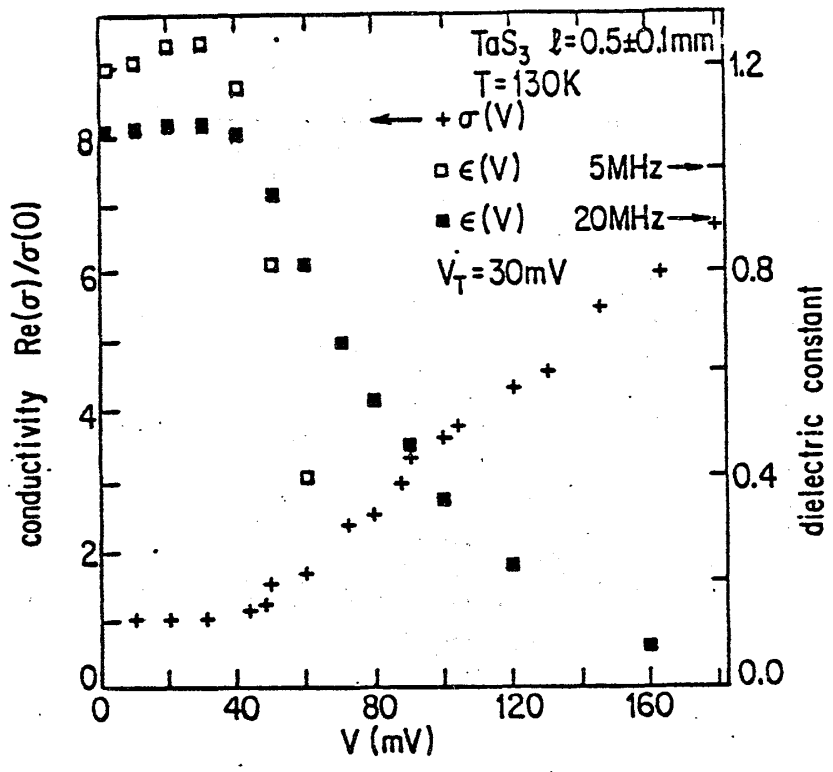

Figure 19

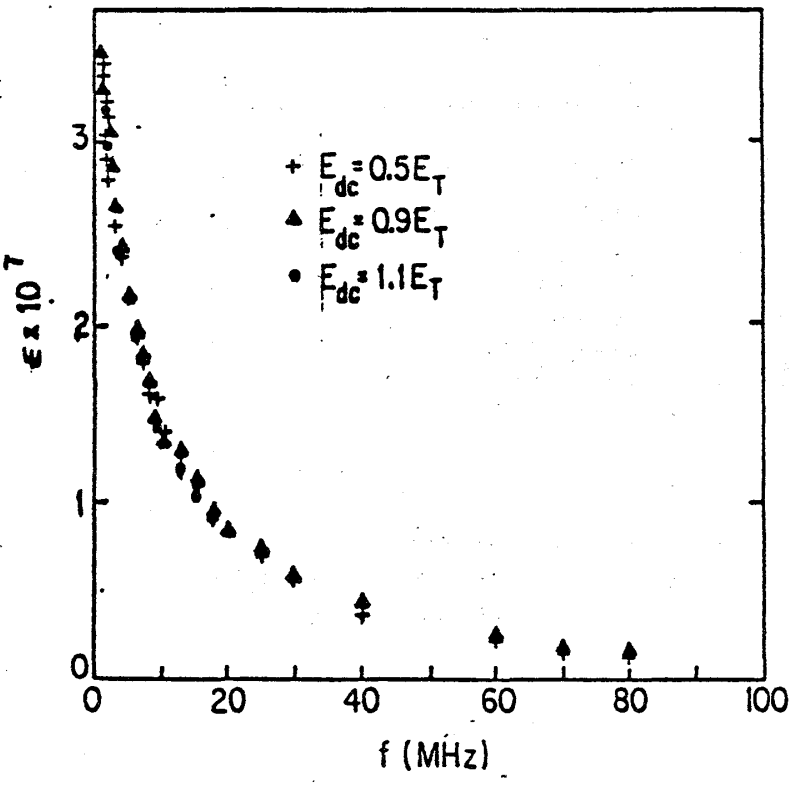

Figure 20

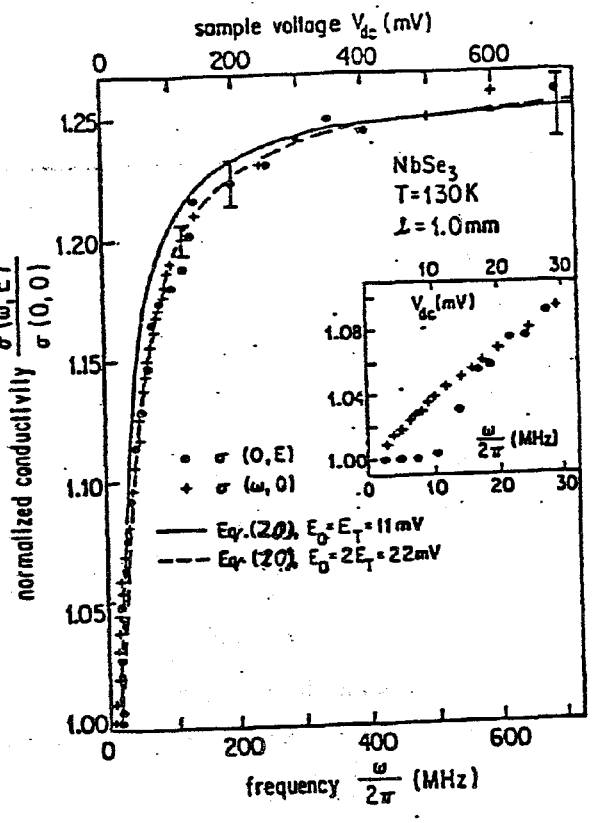

Figure 21

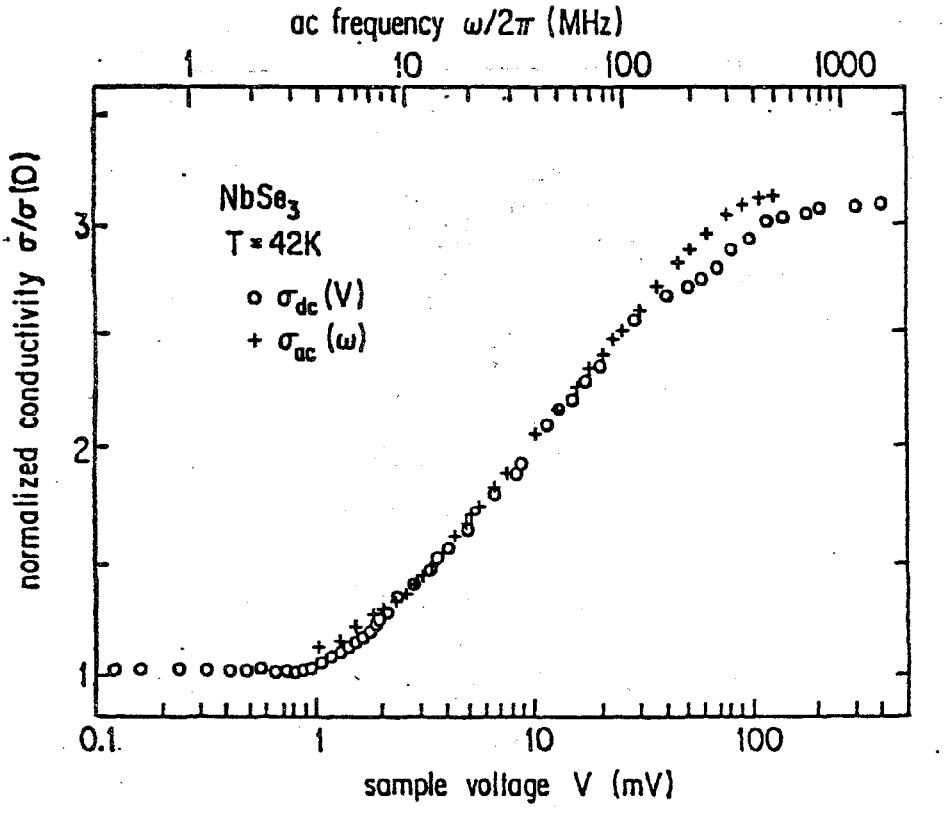

Figure 22

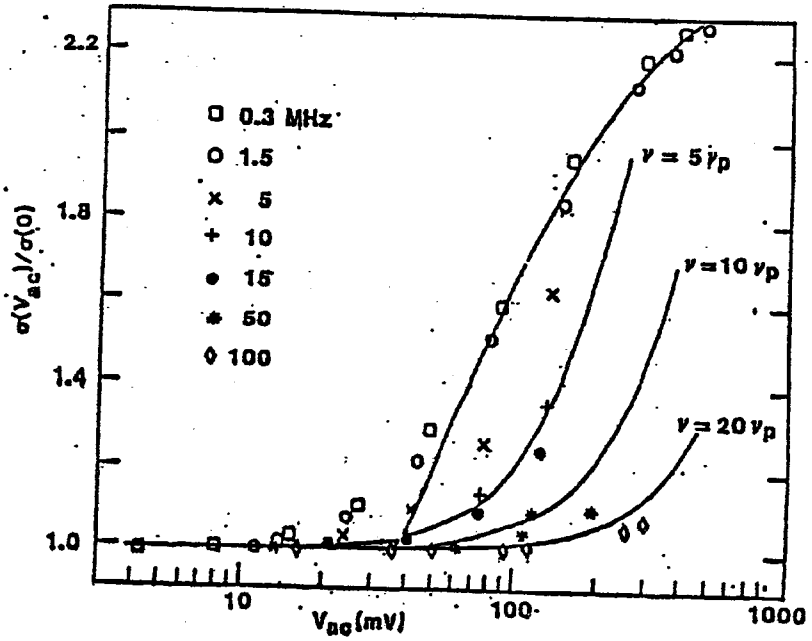

Figure 23

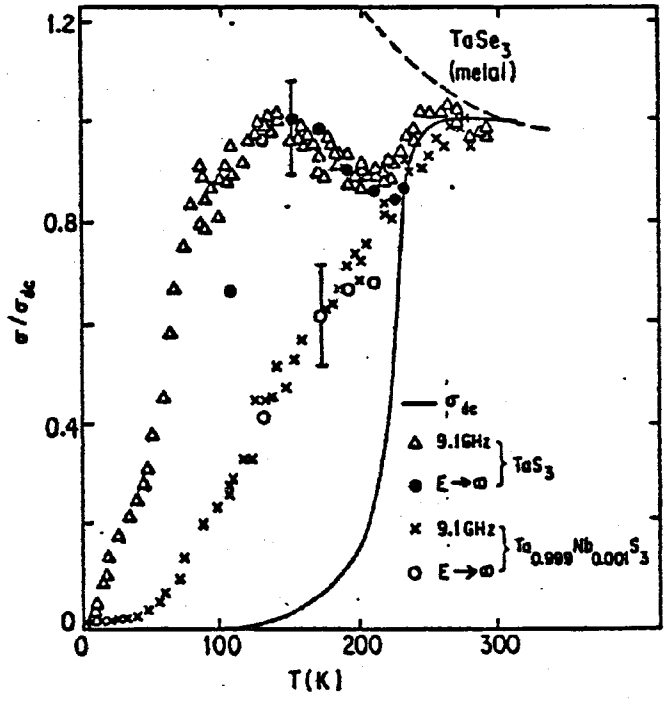

Figure 24